

Nonisothermal Crystallization Kinetics of Linear Bimodal-Polyethylene (LBPE) and LBPE/Low-Density Polyethylene Blends

Jungang Gao, Maoshang Yu, Yanfang Li, Zhiting Li

Department of Polymer Science, College of Chemistry and Environmental Science, Hebei University, Baoding 071002, China

Received 12 August 2002; accepted 12 November 2002

ABSTRACT: Nonisothermal crystallization kinetics of linear bimodal-polyethylene (LBPE) and the blends of LBPE/low-density polyethylene (LDPE) were studied using DSC at various scanning rates. The Avrami analysis modified by Jeziorny and a method developed by Mo were employed to describe the nonisothermal crystallization process of LBPE and LBPE/LDPE blends. The theory of Ozawa was also used to analyze the LBPE DSC data. Kinetic parameters such as, for example, the Avrami exponent (n), the kinetic crystallization rate constant (Z_c), the crystallization peak temperature (T_p), and the half-time of crystallization ($t_{1/2}$) were determined at various scanning rates. The appearance of double melting peaks and double crystallization peaks in the

heating and cooling DSC curves of LBPE/LDPE blends indicated that LBPE and LDPE could crystallize, respectively. As a result of these studies, the Z_c of LBPE increases with the increase of cooling rates and the T_p of LBPE for LBPE/LDPE blends first increases with increasing LBPE content in the blends and reaches its maximum, then decreases as the LBPE content further increases. © 2003 Wiley Periodicals, Inc. *J Appl Polym Sci* 89: 2431–2437, 2003

Key words: linear bimodal polyethylene; low-density polyethylene; blends; nonisothermal crystallization kinetics; differential scanning calorimetry (DSC)

INTRODUCTION

Polyethylene (PE) is currently the most widely used commercial polymer in the world.¹ Because of its specific properties, such as high chemical and mechanical resistance, easy processibility, low specific gravity, and cost, the industrial PE market is still growing. New grades of PE with high performance are eagerly awaited. Bimodal PE,^{2,3} which exists in high and low molecular weight components simultaneously in similar concentrations, is the latest PE grade. Because its properties are superior to those of unimodal PE, it has dominated the domestic markets related to high-density polyethylene (HDPE) film products (e.g., shopping and garbage bags) as well as products from blow molding (e.g., milk and shampoo bottles) in recent years.

Investigations of the kinetics of polymer crystallization⁴ are significant both theoretically and practically. Most frequently, the investigations are conducted under isothermal conditions because of the convenience

of the theoretical treatment of the data. In fact, linear bimodal-polyethylene (LBPE) usually undergoes a nonisothermal crystallization process, especially in practical processing. As a result, a study on the nonisothermal crystallization process of LBPE and LBPE/low-density polyethylene (LDPE) blends is meaningful. However, so far, there are few reports on the nonisothermal crystallization of LBPE and LBPE/LDPE blends.

In this study the Avrami analysis modified by Jeziorny and a method developed by Mo were employed to describe the nonisothermal crystallization process of LBPE and LBPE/LDPE blends. The theory of Ozawa was also used to analyze the LBPE DSC data at various scanning rates. As a result, the crystallization behavior of LBPE and LBPE/LDPE blends obeys the Avrami equation modified by Jeziorny and Mo. Ozawa theory can be used to determine the crystallization behavior of LBPE, but the overall crystallization process does not obey the Ozawa equation.

EXPERIMENTAL

Materials

The linear bimodal-polyethylene (LBPE, FB2230) used was purchased from Northern European Chemical Industry Co.; low-density polyethylene (LDPE, FD0274) was purchased from Qatar Petrochemical Co. Ltd. (Qatar).

Correspondence to: J. Gao (gaojg@mail.hbu.edu.cn).
Contract grant sponsor: Natural Science Foundation, Hebei Province, China; contract grant number: 201068.
Contract grant sponsor: Educational Science Foundation, Hebei Province, China; contract grant number: 2000105.

Preparation of LBPE and lbpe/lbpe blends

The blending method of LBPE with LDPE is a conventional process. The ratios of LBPE/LDPE (particle form) were 100/0; 80/20; 60/40; 40/60; 20/80; 0/100 by weight, respectively. All components were first mixed in a mixer and then milled on a laboratory two-roll mill at the temperatures of $140 \pm 1^\circ\text{C}$ for 10 min. Plates approximately 2 mm thick were pressed at a temperature of $140 \pm 1^\circ\text{C}$.

Thermal measurements

Thermal measurements were made on a CDR-4P calorimeter (Shanghai Exact Science Instrument Co., Ltd., China) with a sample weight of about 8 mg under a nitrogen atmosphere. The temperature and melting enthalpy were calibrated with standard indium. To erase the previous thermal history, the samples were encapsulated into aluminum pans and were heated to 180°C and kept for 5 min. They were then cooled to room temperature at different constant cooling rates (D) (i.e., D values of 3, 6, 10, and $12^\circ\text{C}/\text{min}$, respectively) and the heat flow during crystallization was recorded as a function of time or temperature. For the heating process, the samples that had been cooled at a $10^\circ\text{C}/\text{min}$ cooling rate from 180°C to room temperature were heated at different constant rates (i.e., D values of 6, 10, 15, and $20^\circ\text{C}/\text{min}$, respectively) from room temperature to 180°C again, and the heat flow during melting was recorded.

RESULTS AND DISCUSSION

Theories of kinetic parameter determinations

The relative degree of crystallinity (X_t)⁴ as a function of temperature is defined as

$$X_t = \frac{\int_{T_0}^T (dH_c/dT) dT}{\int_{T_0}^{T_\infty} (dH_c/dT) dT} \quad (1)$$

where T_0 and T_∞ are the onset and end of crystallization temperature, respectively. dH_c/dT is the heat flow at temperature T .

The time of the fastest crystallization (t_{\max}) is the time the crystallization starts to the appearance of the crystallization peak. As a function of temperature (T) and cooling rate (D), t_{\max} is defined as

$$t_{\max} = \frac{T_p - T_0}{D} \quad (2)$$

where T_p is the temperature of crystallization peak.

The half-time of crystallization ($t_{1/2}$)⁵ is the required time for 50% crystallization. The smaller the value of $t_{1/2}$, the faster the crystallization rate.

The degree of crystallinity (X_c)⁶ is defined as

$$X_c = \frac{\Delta H_f}{\Delta H_f^0} \quad (3)$$

where ΔH_f and ΔH_f^0 are the melting enthalpies of PE sample and 100% crystallization PE, respectively. $\Delta H_f^0 = 273 \text{ J/g}$.⁶ ΔH_f is acquired by the integral area of a DSC heating curve.

The kinetic parameters of nonisothermal crystallization were determined on the basis of the simplified assumption that crystallization occurs under constant temperature. In this case, the Avrami equation can be used^{7,8}:

$$1 - X_t = \exp(-Z_t t^n) \quad (4)$$

or

$$\log[-\ln(1 - X_t)] = n \log t + \log(-Z_t) \quad (5)$$

where X_t is the relative degree of crystallinity at crystallization time t , which can be obtained by the following equation:

$$t = \frac{T_0 - T}{D} \quad (6)$$

where T is the temperature of crystallization time t and D is the cooling rate. From eqs. (5) and (6) we obtain eq. (7):

$$\log[-\ln(1 - X_t)] = \log(-Z_t) + n \log\left(\frac{T_0 - T}{D}\right) \quad (7)$$

where n is the Avrami exponent, which depends on the type of nucleation and growth dimension; and the parameter Z_t is a composite rate constant that involves both nucleation and growth rate parameters. The Avrami exponent (n) and crystallization rate constant (Z_t) can be obtained from the slope and intercept of the line in the plot of $\log[-\ln(1 - X_t)]$ versus $\log[(T_0 - T)/D]$. Considering the effect of the cooling rate, Z_t is corrected by the cooling rate⁹:

$$\log(-Z_c) = \frac{\log(-Z_t)}{D} \quad (8)$$

where Z_c is the kinetic crystallization rate constant.

Ozawa¹⁰ extended the Avrami equation to the nonisothermal condition. Assuming that the nonisothermal crystallization process may be composed of

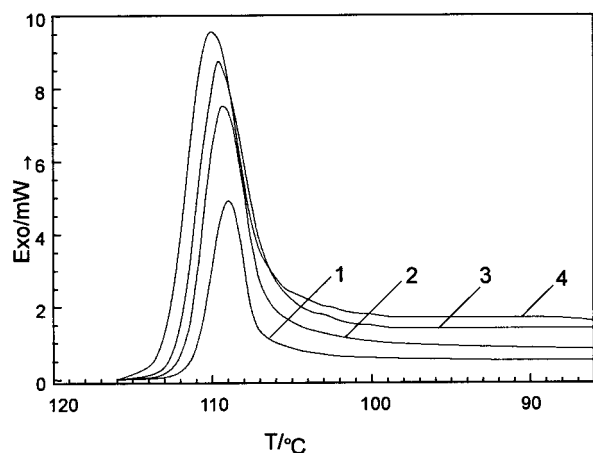


Figure 1 DSC thermograms of LBPE at different cooling rates. 1, 3°C/min; 2, 6°C/min; 3, 10°C/min; 4, 12°C/min.

infinitesimally small isothermal crystallization steps, the following equation was derived:

$$1 - X_t = \exp[-K(T)/D^m] \quad (9)$$

or

$$\log[-\ln(1 - X_t)] = \log K(T) - m \log D \quad (10)$$

where $K(T)$ is the function of cooling rate and m is the Ozawa exponent, which is dependent on the dimension of the crystal growth.

A method developed by Mo¹¹ was also employed to describe the nonisothermal crystallization for comparison. For the process, physical variables relating to the process are the relative degree of crystallinity X_t , cooling rate D , and crystallization temperature T . Both the Ozawa and Avrami equations can relate these variables as follows:

$$\log Z_t + n \log t = \log K(T) - m \log D \quad (11)$$

and by rearrangement,

$$\log D = \log F(T) - a \log t \quad (12)$$

where $F(T) = [K(T)/Z_t]^{1/m}$ refers to the cooling rate value, which must be chosen within unit crystallization time when the measured system amounts to a certain relative degree of crystallinity; a is the ratio of

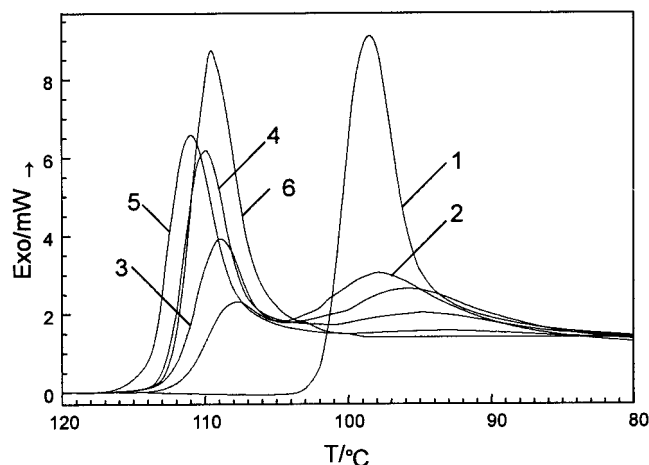


Figure 2 DSC thermograms of LBPE/LDPE blends at 10°C/min cooling rates. LBPE/LDPE: 1, 0/100; 2, 20/80; 3, 40/60; 4, 60/40; 5, 80/20; 6, 100/0.

the Avrami exponent n to the Ozawa exponent m ($a = n/m$). According to eq. (12), at a given relative degree of crystallinity, plotting $\log D$ versus $\log t$ yields a linear relationship between $\log D$ and $\log t$. The data of kinetic parameter $F(T)$ and a can be estimated from the intercept and slope.

Crystallization behavior of LBPE and LBPE/LDPE blends

The crystallization exotherms of LBPE at different cooling rates are presented in Figure 1. From these curves, some useful data can be obtained for describing their nonisothermal crystallization behavior, such as the peak temperature (T_p), relative degree of crystallinity (X_t), and the half-time of crystallization ($t_{1/2}$); values of the parameters determined are given in Table I. It is clearly seen from Figure 1 that T_p shifts, as expected, to a higher temperature when the cooling rate increases, which is attributed to the lower time scale that allows the polymer to crystallize as the cooling rate increases, thus requiring a higher undercooling to initiate crystallization. On the other hand, when the specimens are cooled fast, the motion of LBPE molecules is not able to follow the cooling temperature.

The crystallization exotherms of the pure components and blends at 10°C/min cooling rate are shown

TABLE I
Parameters of LBPE Sample During Nonisothermal Crystallization Process

D (°C/min)	T_0 (°C)	T_p (°C)	t_{max} (S)	$t_{1/2}$ (S)	$\log(-Z_t)$	n	$-Z_c$
3	116	109	140	190	3.167	-1.594	0.294
6	116	109.4	66	95	3.119	-0.678	0.771
10	116	109.5	39	57	3.121	0.0147	1.003
12	116	110	30	47.5	3.121	0.261	1.051

TABLE II
Nonisothermal Crystallization Kinetic Parameters of Blends Sample at 10°C/min Cooling Rates

LBPE/LDPE	T_0 (°C)	T_{p1} (°C)	T_{p2} (°C)	t_{max} (S)	$t_{1/2}$ (S)
0/100	104	—	98.6	32.5	43.2
20/80	115	107.5	97.7	45	90
40/60	116	109	95.8	42	84
60/40	116	110	94.8	36	73.2
80/20	117	111	92.4	36	59.4
100/0	116	109.5	—	39	54

in Figure 2 and the values of the parameters determined are given in Table II. From the curves of Figure 2, it is clearly seen that the LBPE/LDPE blends have two peaks (the first one T_{p1} and the second one T_{p2}), although the crystallization peak temperature (T_{p1}) of the blends was influenced by the LDPE content. The T_{p1} value of the blends first increases with increasing LDPE content and reaches its maximum at 20 wt %, after which the value decreases as the LDPE content is further increased. This behavior has been attributed to a possible interplasticizing action caused by some molecules of LDPE acting as a diluent within the crystalline regions of LBPE when the LDPE content is over 40 wt % in the blends. Therefore, compared with the T_{p1} of pure components, the blends have lower crystallization peak temperatures (T_{p1}). However, when the LDPE content is about 20 wt % in the blends, the blends have higher T_{p1} compared to that of pure LBPE, which can be attributed to a possible prompting action caused by a slightly higher molecular weight component of LDPE acting as a nucleating agent. The second peaks of the blends are all wide and the T_{p2} value of the blends increases with increasing LDPE content.

Nonisothermal crystallization kinetics of LBPE and LBPE/LDPE blends

Figure 3 shows the relative degree of crystallinity of

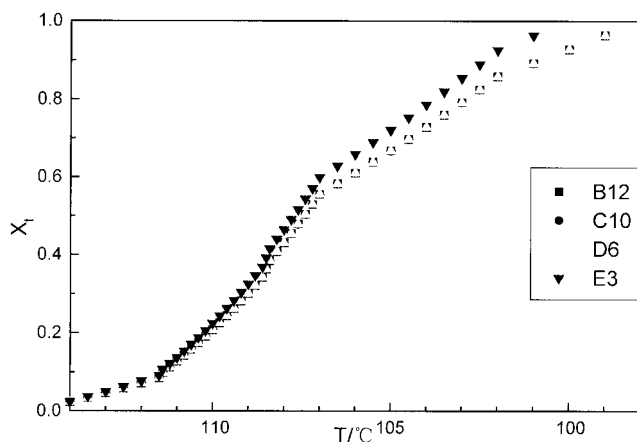


Figure 3 Plots of X_t versus T for crystallization of LBPE. B, 12°C/min; C, 10°C/min; D, 6°C/min; E, 3°C/min.

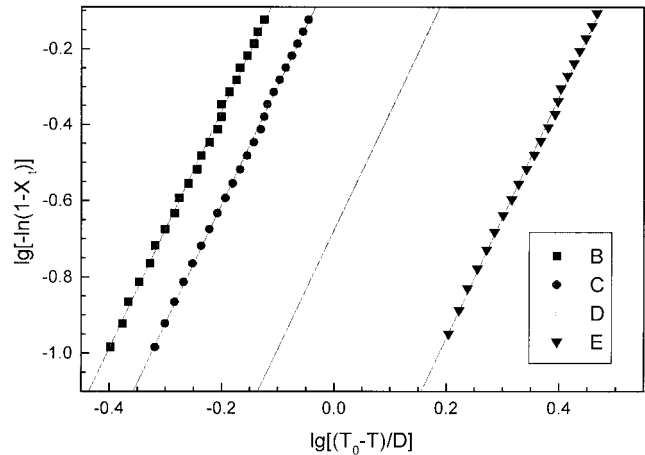


Figure 4 Plots of $\log[-\ln(1 - X_t)]$ versus $\log[(T_0 - T)/D]$ for crystallization of LBPE. B, 12°C/min; C, 10°C/min; D, 6°C/min; E, 3°C/min.

LBPE as a function of temperature at different cooling rates. It can be seen that all these curves have the same S-shape.

Figure 4 shows a good linear relationship when $\log[-\ln(1 - X_t)]$ is plotted versus $\log[(T_0 - T)/D]$ for LBPE at each cooling rate. Two adjustable parameters, Z_t and n , can be obtained by a linear regression. The Z_t and n parameters do not have the same physical meaning as in the isothermal crystallization because the temperature changes constantly in nonisothermal crystallization. This affects the rates of both nuclei formation and spherulite growth ascribed to their temperature dependency. Therefore Z_t must be calibrated by the Jeziorny method. The results are listed in Table I. It is clearly seen from Table I that the simplified assumption that crystallization occurs under constant temperatures is satisfied. That the value of n scarcely changes with the variation of the cooling rates suggested that the nonisothermal crystallization of LBPE

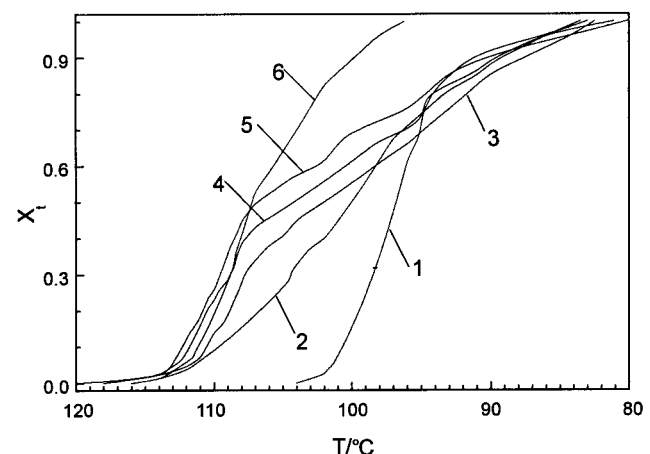


Figure 5 Plots of X_t versus T for crystallization of LBPE/LDPE blends. LBPE/LDPE: 1, 0/100; 2, 20/80; 3, 40/60; 4, 60/40; 5, 80/20; 6, 100/0.

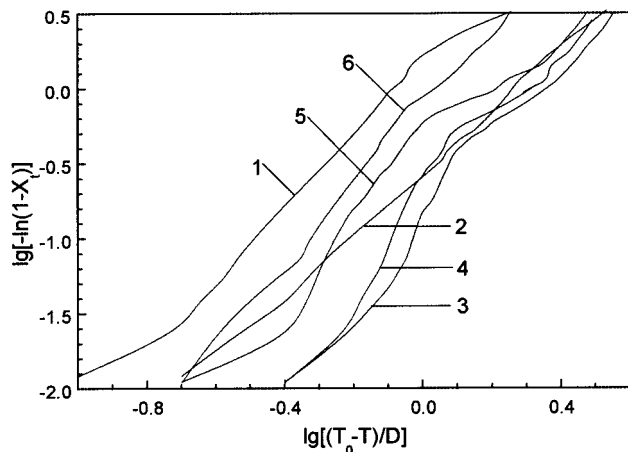


Figure 6 Plots of $\log[-\ln(1 - X_t)]$ versus $\log[(T_0 - T)/D]$ for crystallization of LBPE/LDPE blends. LBPE/LDPE: 1, 0/100; 2, 20/80; 3, 40/60; 4, 60/40; 5, 80/20; 6, 100/0.

corresponds to a tridimensional growth with heterogeneous nucleation because of the higher molecular weight components in LBPE. The value of Z_c increases with increases in the cooling rates for LBPE.

By the same method and at 10°C/min cooling rate, we can also obtain the results shown in Figures 5 and 6. Figure 5 shows the relative degree of crystallinity as a function of temperature and Figure 6 gives the plots of $\log[-\ln(1 - X_t)]$ versus $\log[(T_0 - T)/D]$ for different LDPE content blends. When the LDPE content changes from 40 to 80 wt % in the blends, as seen from Figure 6, the plots of $\log[-\ln(1 - X_t)]$ versus $\log[(T_0 - T)/D]$ no longer demonstrate a good linear relationship and the Avrami equation modified by Jeziorny is no longer adequate to describe the crystallization process of the blends.

Figure 7 shows the results for LBPE according to Ozawa's method. When the crystallization tempera-

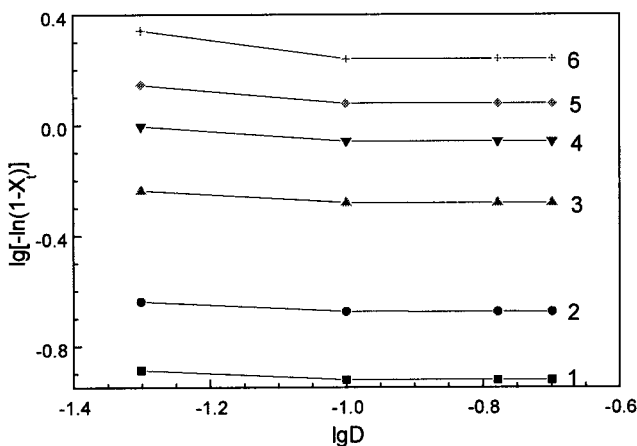


Figure 7 Ozawa plots of $\log[-\ln(1 - X_t)]$ versus $\log D$ for crystallization of LBPE at different crystallization temperatures. 1, 111°C; 2, 110°C; 3, 108°C; 4, 106°C; 5, 104°C; 6, 102°C.

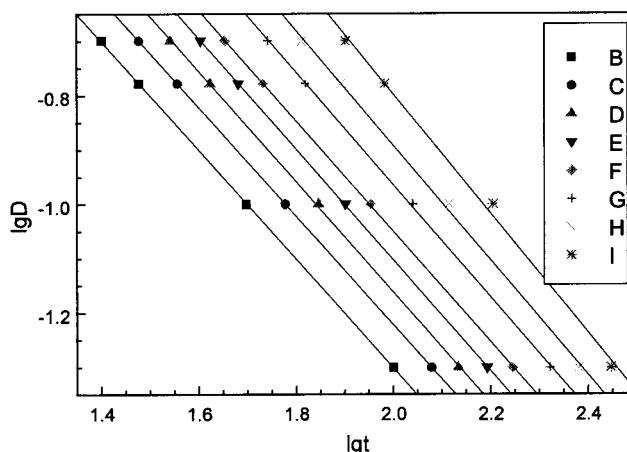


Figure 8 Plots of $\log D$ versus $\log t$ for LBPE at each given relative crystallization. X_t : B, 0.11; C, 0.19; D, 0.28; E, 0.41; F, 0.53; G, 0.64; H, 0.76; I, 0.89.

tures are lower than 109°C, the curvature in Figure 8 prevents an accurate analysis of nonisothermal crystallization data. This can be explained that, at a given temperature, the crystallization process at different cooling rates are at different stages, that is, the lower cooling rate process is toward the end of the crystallization process, whereas at the higher cooling rate, the crystallization process is at an early stage. Although Ozawa's approach can be used to describe the nonisothermal crystallization behavior of LBPE, the variation in the slope with temperature (Fig. 7) means that the parameter m is not a constant during crystallization and that Ozawa's approach is not a good method to describe the nonisothermal crystallization process of LBPE.

The method developed by Mo was also employed to describe the nonisothermal crystallization for comparison. According to eq. (12), at a given relative degree of crystallinity, plotting $\log D$ versus $\log t$ (Fig. 8) yields a linear relationship. The data of kinetic parameter $F(T)$ and a estimated from the intercept and slope for LBPE are listed in Table III.

It can be seen from Table III that the values of $F(T)$ systematically increase with the increment of X_t values for LBPE. The values of a vary from 1.000 to 1.099.

TABLE III
Nonisothermal Crystallization Parameters of LBPE
Sample at Each Given Relative Crystallization

X_t	a	$\log[F(t)]$	$F(t)(K \cdot S^{m-1})$
0.11	1.003	0.704	5.063
0.19	1.000	0.778	6.004
0.28	1.017	0.871	7.434
0.41	1.021	0.940	8.700
0.53	1.017	0.984	9.634
0.64	1.036	1.108	12.820
0.76	1.057	1.222	16.670
0.89	1.099	1.401	25.150

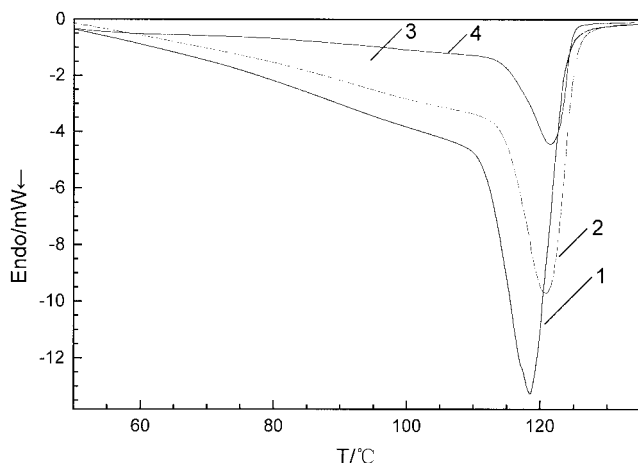


Figure 9 DSC thermograms of LBPE at different heating rates. 1, 20°C/min; 2, 15°C/min; 3, 10°C/min; 4, 6°C/min.

It is clear that this approach is successful in describing the nonisothermal process of LBPE.

Melting curves of LBPE and LBPE/LDPE blends

Figure 9 shows DSC thermograms of LBPE at different heating rates. From these curves, some useful data can be obtained for describing their nonisothermal melting behavior, such as the peak temperature (T_p) at which LBPE has the fastest melting rate, and the melting enthalpy (ΔH_f), which can be acquired by the integral area of a DSC heating curve and the sample degree of crystallinity (X_c). The values of the parameters determined are given in Table IV. It is clearly seen from Table IV and Figure 9 that the variation of parameters for LBPE at different heating rates corresponds with that at different cooling rates.

Figure 10 shows DSC thermograms of blends with different LDPE contents at a heating rate of 10°C/min, and Table V gives some parameters of DSC heating curves. From Figure 10 and Table V, we can see that the variation of parameters for blends of different LDPE content also corresponds with that at a cooling rate of 10°C/min.

CONCLUSIONS

The Ozawa analysis failed to provide an adequate description of the nonisothermal crystallization of

TABLE IV
Parameters of LBPE Sample During Nonisothermal Heating Process

D (°C/min)	T_p (°C)	ΔH_f (J/g)	X_c (%)
20	118.6	145.7	53.4
15	120.9	122.4	44.8
10	121.5	115.9	42.5
6	121.5	118.1	43.2

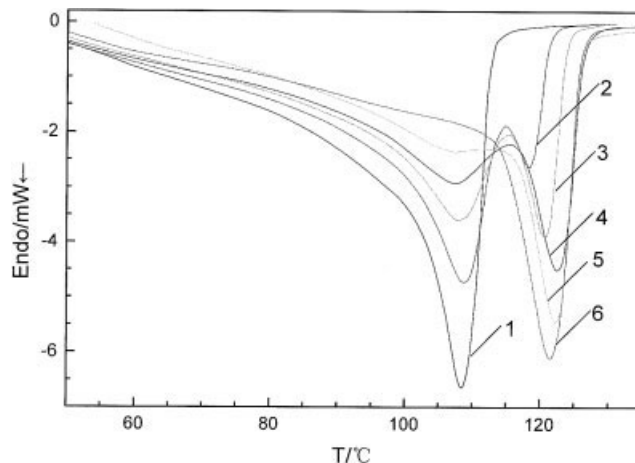


Figure 10 DSC thermograms of LBPE/LDPE blends at 10°C/min heating rates. LBPE/LDPE: 1, 0/100; 2, 20/80; 3, 40/60; 4, 60/40; 5, 80/20; 6, 100/0.

LBPE because of the comparisons of different stages of crystallization at different cooling rates. The Avrami analysis modified by Jeziorny and a method developed by Mo were successful in describing the nonisothermal crystallization process of LBPE. That the value of n scarcely changes with the variation of the cooling rates suggested that the nonisothermal crystallization of LBPE corresponds to a tridimensional heterogeneous growth, and the values of Z_c increase incrementally with the cooling rates for LBPE.

The Avrami equation modified by Jeziorny is no longer adequate to describe the crystallization process of the LBPE/LDPE blends. The appearance of double melting peaks and the double crystallization peaks in the heating or cooling DSC curves of LBPE/LDPE blends indicated that the LBPE and LDPE could crystallize, respectively. The blending of LBPE with LDPE can influence the crystallization peak temperature (T_p) of LBPE. The T_p of LBPE first increases with increasing LDPE content in the blends and reaches its maximum at 20 wt %, after which it decreases as the LDPE content is further increased.

The authors gratefully acknowledge the financial support from the Natural Science Foundation (No. 201068) and Ed-

TABLE V
Parameters of LBPE/LDPE Blends Sample During Nonisothermal Heating Process

LBPE/LDPE	T_{p1} (°C)	T_{p2} (°C)	ΔH_f (J/g)	X_c (%)
0/100	108.5	—	152.8	56.0
20/80	108.6	118.4	140.6	51.5
40/60	107.9	120.5	131.5	48.2
60/40	107.5	122.4	131.2	48.2
80/20	107.3	122.4	140.7	51.5
100/0	—	121.5	115.9	42.5

ucational Science Foundation (No. 2000105) of Hebei Province, China.

References

1. Mori, H.; Ohnishi, K.; Terano, M. *Macromol Chem Phys* 1998, 199, 393.
2. China Plastics Industry Editorial office. *China Plast Industry* 2001, 29, 2.
3. Fu, J. J.; Min W. W. *Petrochem Technol Appl China* 2000, 18, 112.
4. Kong, X. H.; Yang, X. N.; Li, C.; Zhao, X. G.; Zhou, E.; Ma, D. *Eur Polym J* 2001, 37, 1855.
5. Zhang, Z. Y.; Wu, S. Z.; Du Y. H.; Cao, Z. L. *Chin J Polym Sci* 1991, 9, 319.
6. Dong, Y. M. *The Practical Analysis Technology of Polymer Materials*; Petrochemical Industry Press: Beijing, 1997; p. 293.
7. Xu, X. R.; Xu, J. T.; Chen, L. S.; Liu, R. W.; Feng, L. X. *J Appl Polym Sci* 2001, 80, 124.
8. Xu, W.; Ce, M.; He, P. *J Appl Polym Sci* 2001, 82, 2281.
9. Jeziorny, A. *Polymer* 1978, 19, 1142.
10. Ozawa, T. *Polymer* 1971, 12, 150.
11. Liu, T. X.; Mo, Z. S.; Wang, S. E.; et al. *Polym Eng Sci* 1997, 37, 568.